

# STUDY OF THE EVOLUTION OF ARTIFICIAL DEFECTS ON THE SURFACE OF NIOBIUM DURING ELECTROCHEMICAL AND CHEMICAL POLISHING

L. Monaco<sup>#</sup>, P. Michelato, INFN Milano - LASA, Segrate, Italy  
 C. Pagani, Università degli Studi di Milano & INFN, Segrate, Italy  
 A. Navitski, J. Schaffran, W. Singer, DESY, Hamburg, Germany  
 A. Prudnikava, Y. Tamashevich, University of Hamburg, Hamburg, Germany

## Abstract

The presence of defects on the inner surface of Nb superconducting RF structures might limit its final performance. For this reason, strict requirements are imposed during mechanical production of the cavities, specifically on the quality control of the inner surface of components, to avoid the presence of defects or scratches. Nevertheless, some defects may remain also after control or can arise from the following production steps. Understanding the evolution of the defect might shine new insight on its origin and help in defining possible repair techniques.

This paper reports the topographical evolution of defects on a Nb sample polished with the standard recipe used for the 1.3 GHz cavities of the EXFEL project. Various artificial defects of different shape, dimensions, and thicknesses/depths, with geometrical characteristics similar to the one that may occur during the machining and handling of cavities, have been “ad hoc” produced on the sample of the same material used for the cell fabrication. Analysis shows the evolution of the shape and profile of the defects at the different polishing steps.

## INTRODUCTION

One meaningful aspect in the niobium cavities production is the quality of the inner surface that must be treated with particular care. Indeed, it is well known that the presence of contaminants, dusts, inclusions and surface defects (scratches, bumps, holes, etc.) on the RF inner Nb surface can limit the cavities performances during their operation [1].

Hence, for the EXFEL cavities production, a strict quality control is applied not only to the raw material used for the fabrication of the resonators [2], but also during all preparation steps of the inner surface of Nb cavities [3].

However, despite the strict quality control, mechanical defects can be introduced during the cavity production cycle. Scratches, bumps or holes may occur during the mechanical production of subcomponents, or can be originated by not proper handling or caused by accident during the various treatment steps. The understating of these defects evolution during the following electrochemical (Electro Polishing, EP) and chemical (Buffered Chemical Polishing, BCP) treatments is important to evaluate which kind of defects could be

critical for the final resonator performances and which one can be considered as a low risk.

Different equipment developed and built at the laboratories and at the industries are in operation for the quality control of inner surface of the resonators. For EXFEL, inspections are performed not only during the cavity production but also after their cold test if the cavity is not performing as expected [4]. Even if these systems allow detecting and also curing defects with good result (i.e. [5]), the evaluation of the defect evolution is not yet well studied and can be a powerful tool to limit this kind of “cure” only to defects that represent a real high risk for the performance of cavities.

In this paper, we present preliminary results of a study of the evolution during EP/BCP treatments of artificial defects mechanically produced on a Nb sample that are representative of the ones that could be found on the inner surface of resonators. The analysis was started few years ago [6] and is still ongoing with an improved diagnostic. Those measurements gave information on the evolution of main geometrical parameters of defects (i.e. diameter, height) with a rough estimation of their profiles.

This year, in collaboration with DESY, we started a new series of measurements on a new Nb sample, prepared with artificial defects as done in the past. All operation concerning the preparation of the sample and the production of artificial defects, as well as all etching treatments have been performed at LASA, while scanning, images of defects and also profile and roughness measurements before and after each treatment steps have been done at DESY. The aim of these new measurements is to have a complete analysis of defect evolution under EP and BCP treatments, with particular care on the profile evolution, of the smoothness of the edges of the defects and precise measurements of the depth and roughness evolution.

## EXPERIMENTAL SET-UP

### *Sample Preparation and Production of Artificial Defects*

A sample (50mm x 85mm x 3mm) machined from a Nb sheet used for the production of cavities has been cleaned with pure ethanol, dried and BCP (1:1:2, HF, HNO<sub>3</sub>, H<sub>3</sub>PO<sub>4</sub>) etched with a total removal of 25 μm, before producing the artificial defects. Figure 1 (left) shows a map of different defects produced on the sample surface.

<sup>#</sup>laura.monaco@mi.infn.it

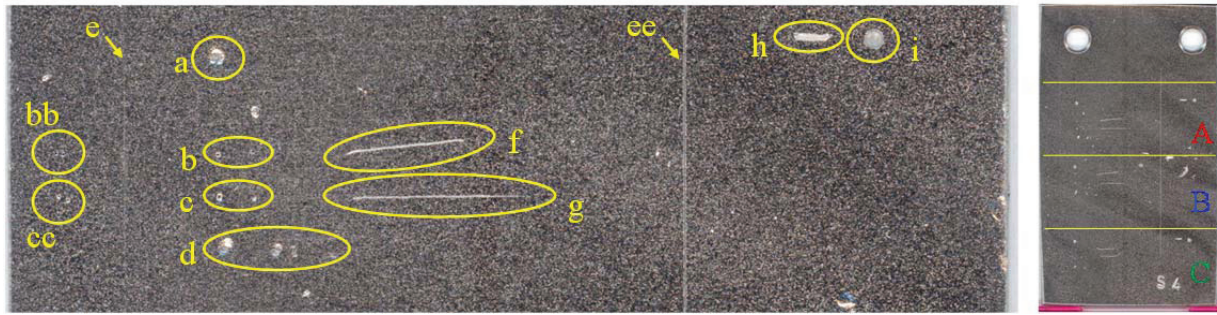


Figure 1: Left: zoom of the map of artificial defects. Right: the three areas with defects.

Table 1 summarized type of defects and tools used for their production.

Table 1: Summary of Produced Defects

Defect code	Tool	Defect Type
a	BS	circular hole
b/bb	RN	circular hole
c/cc	SN	circular hole
d	DH	rhomboid hole
e/ee	C	scratch
f	RN	scratch (and bump)
g	SN	scratch (and bump)
h	SH	bump (and scratch)
i	S	hole

BS: Brass Screw

C: Cutter

RN: Round Needle

SH: Screwdriver Head

SN: Sharp Needle

S: Screw

DH: Drill Head

Holes (a, b, d, i) were produced using several tools at different pressures. Pairs of holes (bb/cc) allow studying possible effects induced by their overlapping. Scratches have been obtained by either pushing a cutter with high and low pressure held in place on the surface (e/ee) or sliding needles of different shapes on the Nb surface (f/g). Bumps have been made pushing a screwdriver head against the surface (h). Bumps are also observable in the tail of the scratches produced with sliding needles (f/g).

Possible influence of etching attacks due to the geometry of the system used for the EP and BCP, has been also considered, replicating the same defects distribution in three areas (A, B, C) of the sample, as shown in Fig. 1 (right).

### EP and BCP System

At LASA, we have a system able to do EP and BCP on small samples. The EP process has been done at constant voltage of 17 V, keeping the EP solution (1:9, HF, H<sub>2</sub>SO<sub>4</sub>) at temperature below 30 °C. During the EP process, we monitor the current to evaluate the total collected charge which is proportional to the material removed [6]. This preliminary estimation of the removal is further checked

by weighting the sample before and after each treatment.

### Equipment for Defect Analysis

The surface analysis was explored using Keyence 3D Laser Scanning Microscope VK-X100, a powerful tool for performing profile, height, area, volume and surface roughness measurements. It utilizes a pinhole confocal optical system with halogen lamp as a light source and a red semiconductor laser for, correspondingly, optical and laser observation. The maximal magnification achieved is x8000 with the display resolution for width measurements of 0.5 μm, and for height measurements, 0.01 μm. The VK-Analyser software allows measuring the height, width, cross-section, angle or radius-of-curvature of any specified line or curved cross-section profile.

### ETCHING ATTACK

To study the effect of surface treatment on defects, we decided to follow the standard recipes used for the EXFEL cavities production. Two recipes are in use: Flash BCP and Final EP [7, 8]. Both recipes consists of a bulk EP (140 μm for Flash BCP and 110 μm for Final EP), followed by 800 °C annealing. They differ in the last surface treatments, where 10 μm are removed with BCP (Flash BCP) and 40 μm are removed by EP (Final EP). Moreover, evolution of defects during BCP is of importance since a light BCP (~10 μm) could be used for recovering poor performance EXFEL cavities [9].

Table 2: EP and BCP Steps

Surface removal	Surface Treatment	Status (treat./scanning)
30 μm	EP	done/done
55 μm	EP	done/done
55 μm <sup>§</sup>	EP	done/to be done
10 μm <sup>*</sup>	BCP	to be done/to be done

<sup>§</sup>The evaluation of removal is still underway (cross check with DESY measurements).

<sup>\*</sup>This treatment is still to be done.

The EP process, corresponding to bulk and Final EP, has been divided in three steps, to be able to follow systematically the topographical evolution of defects

during the full treatment. The last step is a light BCP as used for Flash BCP. Table 2 summarizes the foreseen treatment steps on the Nb sample.

The thickness of the material removed, after each step, on the area with defects is precisely determined by comparing the height difference between the EP exposed area and a small area masked with Fomblin [10] which is EP resistant.

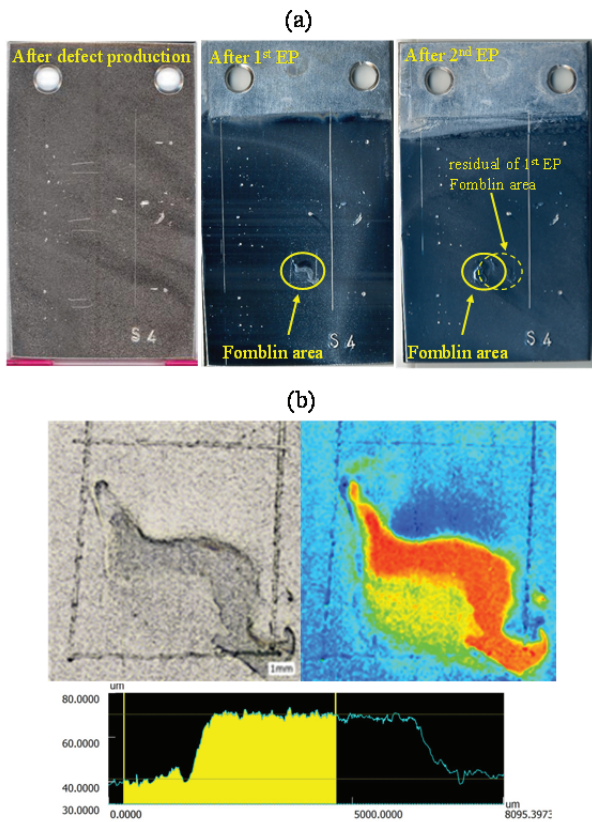


Figure 2: Study of surface removal by EP. (a): optical views of the sample after the defect production, the 1<sup>st</sup> and 2<sup>nd</sup> EP. (b): "Laser", "height" and "profile measurement" images of the Fomblin masked area after the 1<sup>st</sup> EP. Height difference is ~30 μm.

Figure 2(a) shows the scanning of the sample after the defect production and after the 1<sup>st</sup> and 2<sup>nd</sup> EP. In Fig. 2(b) the Fomblin masked area scanned after the 1<sup>st</sup> EP, is shown as an example. The crosscheck of both methods gives the values reported in Table 2. At present, we have performed the first three steps of EP attack. For the first two, all defects have been already measured while measurements after the 3<sup>rd</sup> step are on the way at DESY.

### ANALYSIS AND EVOLUTION OF THE ARTIFICIAL PRODUCED DEFECTS

#### Diameter and Depth Evolution

As a first check, we have compared the available new results with the old ones. As already discussed, since no profile measurements were done at that time, we check the defects evolution only in term of diameter and depth. The general tendency of defects of such type is the

increase in diameter, and decrease of height (or depth), which is well in agreement with our previous data [6].

As an example in Fig. 3 the evolution of diameter versus EP treatments of RN (i.e. b, bb) and of SN (c, cc) - type holes is shown.

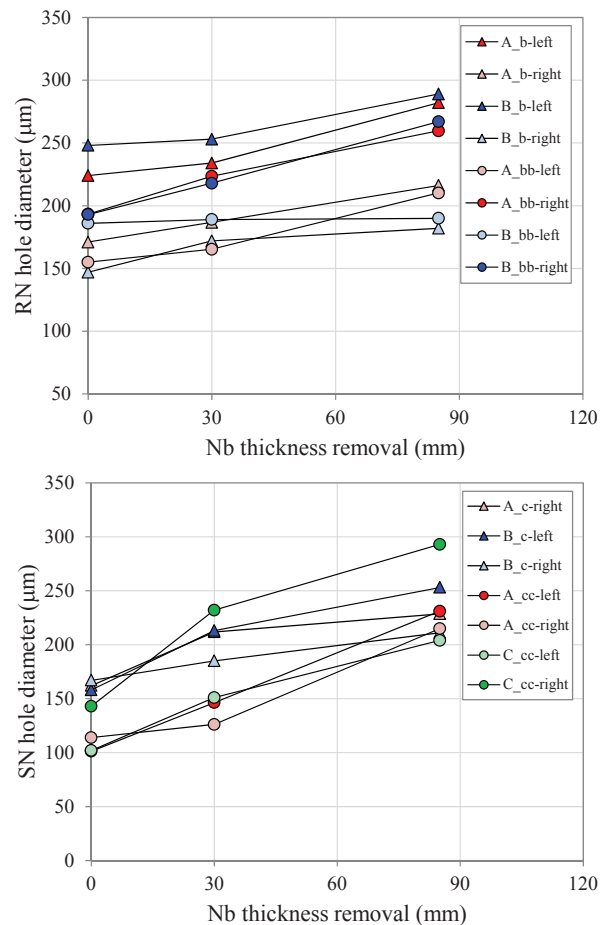


Figure 3: Evolution of diameters of RN and SN type holes. Colours indicate the different sample areas with defects: red (A), blue (B), green (C). Full colours are for defects produced with high pressure, while light colours with low pressure (i.e. A\_cc-left marker in full red, A\_cc-right in light red).

Also the new data show a larger increase of SN type holes diameter with respect to the RN ones during the EP process. Moreover, since the diameter evolution seems to be independent on the position of the defect on the sample, we consider the influence of the EP system geometry to be negligible and, therefore, the EP polishing over the sample surface should be homogeneous.

#### Influence of EP on Defect Shape

The study of profiles evolution is underway on all available defects. Our analysis focuses mainly on the profile evolution and on the smoothness of the edges.

Defect h (obtained with SH tool) is an example of the defect having quite complex shape, since it contains both a protrusion (bump), and a scratch, simultaneously (see Fig. 4).

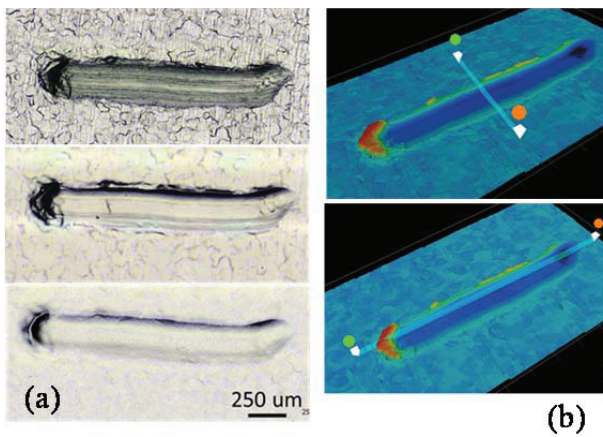


Figure 4: Defect h (SH type defect): (a) optical images; (b) 3D view; 2D profile across (c) and along (d) the defect after EP steps.

The in-plane aspect ratio, Width/Length, is equal to 6, while depth is two orders of magnitude smaller (~12-15 μm). Noteworthy, these dimensions are not affected by EP, though it was removed 85 μm in total. The bump height, however, gradually decreased from 56 to 37 μm (1<sup>st</sup> EP), and to 25 μm (2<sup>nd</sup> EP), i.e. ~33-34% of its initial height upon each EP step. Since the thickness of the removed layers from the sample by the 1<sup>st</sup> and 2<sup>nd</sup> EP was different (30 vs 55 μm), it means that the height of the bump decreases non-linearly with treatment time, and this will be further explored in the future.

Figure 5 shows the evolution of the diameter the RN type hole after EP.

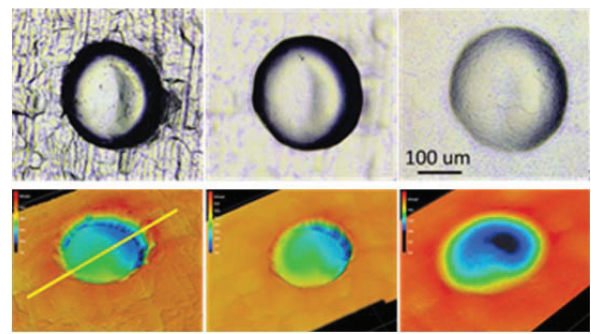


Figure 5: Optical images, 3D views of a RN type hole after different EP steps.

Figure 6 shows a 2D profile through the RN type hole (see Fig. 5 lower left image for cutting plane). It is clearly visible an increase of the edge rounding with EP steps.

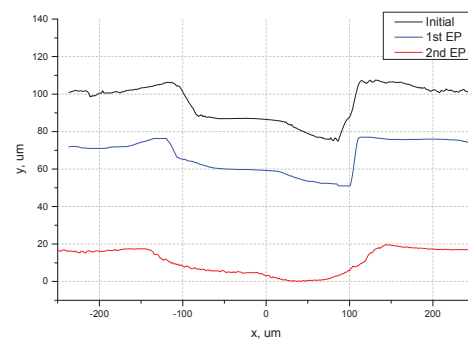


Figure 6: Cross-section profiles after different EP steps for RN type hole defect.

### Simple Model for Profile Evolution

We have developed a simple model to predict the defect profile evolution. It is based on the iterative mesh method and uses only one parameter – the anisotropy of the etching speed. The algorithm defines the local normal vector  $n$  to each point of the profile, and a shift of the profile point in the direction  $s$ . Here,  $s$  is the Hadamard product of  $n$  and of the etching speed vector  $v$ :

$$\begin{pmatrix} s_x \\ s_y \end{pmatrix} = \begin{pmatrix} n_x \\ n_y \end{pmatrix} \odot \begin{pmatrix} v_x \\ v_y \end{pmatrix}$$

The step between iterations was chosen by the common criteria for usual Finite Differences Method (FDM). This model allows the estimation of the etching parameters without the complicated first-principal calculations. For the case shown in Fig. 7 of a SN type hole, for the 1<sup>st</sup> EP the ratio of the etching speed in the normal to the sample plane direction,  $v_y$ , and the etching speed in the tangential to the sample plane direction,  $v_x$ , was found as 1:1.25 while for the 2<sup>nd</sup> EP the ratio is 1:0.5. This can probably indicate that the parameters of EP were different for the two EP steps, at least at the position of this defect.

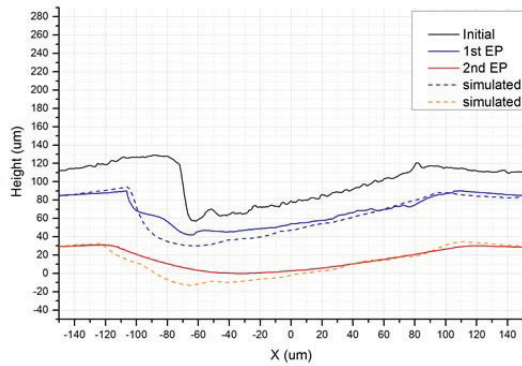


Figure 7: Profile evolution for SN type hole compared to a simple model based on etching speed anisotropy. The deduced anisotropy values are found to be different for the two EP steps.

**Roughness**

The measurement of surface roughness was performed in the plane areas of the sample surface subjected to EP. At each EP step, three different areas of 380 µm x 520 µm were chosen for scanning with laser microscope with x100 objective.

The evolution of the topographic features upon EP is represented by the "height" images shown in Fig. 8. A pronounced smoothing of the grain boundaries is clearly visible after the chemical treatment.

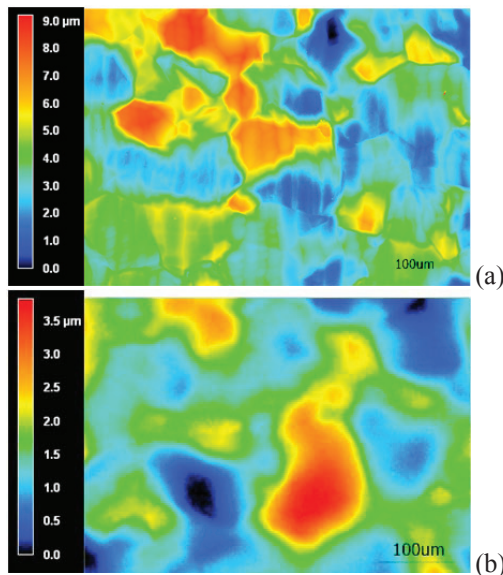


Figure 8: "Height" images of the Nb surface:(a) initial sample and (b) after 2<sup>nd</sup> EP.

In general, roughness noticeably decreases after the 1<sup>st</sup> EP, while subsequent EP doesn't show any pronounced improvement. It is interesting to note that peaks and valleys (compare  $R_p$  and  $R_v$ ) are almost equally smoothed upon EP process. According to  $R_a$  and  $R_q$  values, the mean roughness gets two times smaller after the 1<sup>st</sup> EP.

The measured roughness parameters are summarized in Table 3 where  $R_p$  is the maximum peak height,  $R_v$  is maximum valley depth,  $R_a$  is arithmetic average of absolute values, and  $R_q$  is root mean square.

Table 3: Roughness Parameters [µm]

	$R_p$	$R_v$	$R_a$	$R_q$
Initial	5.4	3.8	1.1	1.4
1 <sup>st</sup> EP	2.4	1.6	0.6	0.7
2 <sup>nd</sup> EP	2.3	1.5	0.5	0.6

**CONCLUSIONS**

We have briefly presented the undergoing measurements aiming to study the defect evolution during the EP treatment, usually done during the preparation of EXFEL cavities.

At present, we are focused on the analysis of defect profiles and dimensions after the first two EP attacks, corresponding to 85 µm surface removal. The preliminary results confirmed the data acquired in our previous work and extend the analysis to profile evolution and roughness estimation. The analysis of the defect evolution after the third EP is now starting at DESY. Afterwards, a light BCP attack (10 µm) is foreseen to complete the study including also the defect evolution obtained by the last step of the Flash BCP recipe.

**REFERENCES**

- [1] H. Padamsee et al., *RF Superconductivity for Accelerators*, John Wiley & Sons, 1998.
- [2] W. Singer et al., "Superconducting cavity material for the European XFEL", *Supercond. Sci. Technol.* 28 (2015) 085014.
- [3] Specification Documents for Production of European XFEL 1.3 GHz SC Cavities. DESY, 2009.
- [4] A. Navitski et al., "Characterization of surface defects on EXFEL series and ILC-HiGrade cavities", MOPB072, these proceedings, SRF'15, Whistler, Canada (2015).
- [5] G. Massaro et al., "Inspection and repair techniques for the EXFEL superconducting 1.3 GHz cavities at Ettore Zanon S.p.A.: methods and results", MOPB094, these proceedings, SRF'15, Whistler, Canada (2015).
- [6] P. Michelato et al., "Evolution of the defects on the Niobium surface during BCP and EP treatments", THPPO091, SRF'09, Berlin, Germany (2009).
- [7] A. Matheisen et al., "Industrialization of European XFEL Preparation Cycle "BCP Flash" at Ettore Zanon Company", TUP056, SRF'13, Paris, France, 2013.
- [8] A. Matheisen et al., "Industrialization of European XFEL Preparation Cycle "Final EP" at Research Instruments Company", MOP040, SRF'13, Paris, France, 2013.
- [9] A. Matheisen et al., "Experiences on retreatment of XFEL series cavities at DESY", MOPB075, these proceedings, SRF'15, Whistler, Canada (2015).
- [10] <http://www.solvay.com/en/markets-and-products/featured-products/Fomblin-PFPE-Lubricants.html>